

Silicon diatom frustules as nanostructured photoelectrodes

Soundarrajan Chandrasekaran^a, Martin J. Sweetman^a, Krishna Kant^b, William Skinner^c, Dusan Losic^b, Thomas Nann^c and Nicolas H. Voelcker^{a*}

^aMawson Institute, University of South Australia, Mawson Lakes Blvd, Adelaide, SA 5095, Australia.

^bSchool of Chemical Engineering, University of Adelaide, Adelaide, SA, 5005, Australia.

^cIan Wark Research Institute, University of South Australia, Mawson Lakes Blvd, Adelaide, SA 5095, Australia.

Supporting Information

Table of contents

Experimental details	3
Figure 1S SEM microscopy	5
Figure 2S High-resolution XPS	6
Figure 3S XPS survey spectra	7
Figure 4S Raman spectra	8
Figure 5S FTIR spectra	9
Figure 6S and 7S Fluorescence labeling of thiol-functionalized diatom silicon	10
References	11

Experimental Section

Magnesiothermic conversion of diatom frustules to silicon replicas

Diatom silica in the form of diatomaceous earth was obtained from Mount Sylvania Pty. Ltd (Queensland, Australia). Purified whole diatom silica frustules without fractures were prepared using our purification and separation process as described elsewhere.¹ 1.25:1 molar ratio of Mg turnings to purified diatom frustules were mixed thoroughly in a tungsten boat, and then heated to 650 °C with a ramping rate of 10 °C per minute and kept for 7 hours in a tube furnace under a flow of industrial grade argon gas (99.995 %). After cooling, the formed products were mixed again and the heating procedure was repeated, to ensure the complete conversion of diatom frustules and no magnesium silicide (Mg_2Si) residues. The MgO/Si composite formed was treated with 2M HCl for 5 hours to remove MgO. Then, any magnesium chloride formed was removed by rinsing with ethanol (5 times). Following rinsing, the silicon diatom frustules were treated with HF (1 HF_(48%aq):2 EtOH) for 2 min to remove any oxide layer formed in the silicon surface. Samples were then washed with ethanol (5 times) and dried in a glove box (high purity argon gas (99.997 %)).

Surface functionalization

Silicon diatom frustules were thermally hydrosilylated in a 1 M ethanolic solution of allyl mercaptan (AM) at 50 °C for 15 hours. They were then purified by washing with absolute ethanol (three times) and vacuum dried, then stored in a glove box.

Electrode fabrication

100 μ L of a 1 mg/mL ethanolic solution of AM hydrosilylated silicon diatom frustules was added to a gold-coated glass slide in a glove box. After drying, this process was repeated 5 times. Then, the surface was then gently washed with distilled water to remove the unbound silicon diatom frustules. The CBD process involved dipping the fabricated electrode in a 0.1 M cadmium nitrate ethanol solution for 5 min, rinsing it with ethanol and then immersing the electrode for another 5 min in a 0.1 M sodium sulphide methanol solution and rinsing it again with methanol. This two-step dipping procedure is considered one CBD cycle. 10 CBD cycles were performed in order to obtain a good coverage of CdS on Si diatom frustules. A control electrode was prepared in the same manner as the test electrode. However, in this case, silicon diatom frustules without AM hydrosilylation were used. The electrode surface was again gently washed with distilled water to remove the unbound silicon diatom frustules.

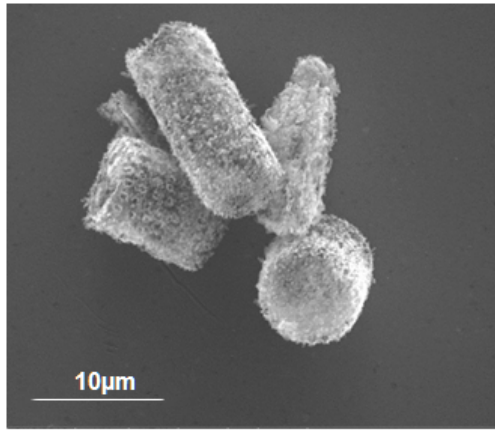
Surface characterization

SEM images and EDXS spectrum were obtained on a FEI Quanta 450 Environmental Scanning Electron Microscope (ESEM). XRD studies of the samples were recorded on a Rigaku – Miniflex 600 Bench top X-ray diffraction (XRD) instrument. Fourier Transform Infrared spectra (FTIR) spectra of the samples were recorded using a Tensor 27 FT-IR spectrometer coupled to a Hyperion 3000 FT-IR microscope. Surface chemical composition state of elements were analysed using a Kratos AXIS Ultra DLD X-ray photoelectron spectrometer, using monochromatic Al K α radiation at 300 W. Spectrometer pass energies of 160 eV and 20 eV were employed for survey and high resolution scans, respectively. Raman spectroscopy of the samples were analysed using a Witec Alpha R confocal Raman microscope. The laser used was a Nd:YAG 532 nm (2.33 eV) laser which has a maximum power at the sample of 30 mW. A 40x objective with a numerical aperture of 0.60 was used. Single spectra were collected with integration times typically between 20 to 30 seconds. Emission intensities of the dye modified silicon diatom frustules were measured on a Perkin-Elmer LS55 luminescence spectrophotometer using an excitation wavelength of 494 nm and

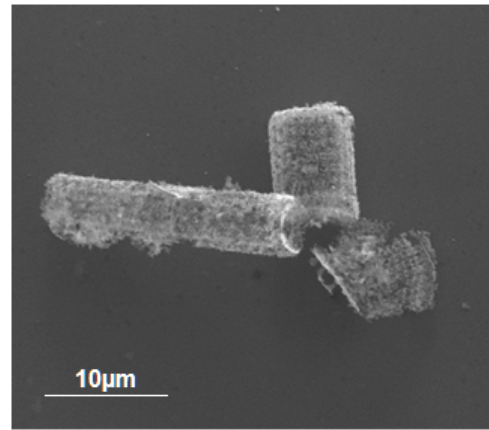
the emission wavelength was recorded between 500-525 nm. Fluorescence microscopy images were recorded with a Nikon Eclipse 50i fluorescence microscope and analyzed by NIS Elements software.

Photocurrent measurements

Irradiation was performed using an Abet Solar Simulator (AM 1.5 – 1 sun) and calibrated against a silicon solar cell (New-Spec). Electrochemical measurements were carried out using a PG 310 potentiostat from HEKA Electronics (Germany). Electrolysis was performed using a sealed three-electrode Teflon photoelectrochemical cell consisting of a Pt counter electrode, an Ag | AgCl 3M KCl reference electrode, and the working electrode. The working electrode was sealed in between two Teflon pieces with a quartz window on one side for illumination. The counter and reference electrodes were inserted in either side (air tight) parallel to the working electrode. The thickness of the Teflon pieces are 1.5 cm each, kept intact in a metal clamp with working electrode. The volume of the electrolyte was 2 mL. The working electrode was illuminated with a light intensity of 100 mW/cm² under air mass 1.5 conditions with short 12 second dark/light cycle to measure the photocurrents as a function of time.



A



B

Figure 1S: SEM images (A and B) of the silicon diatom frustules (*Aulacoseira sp.*) after magnesiothermic conversion process. A molar ratio of 2.5:1 Mg turnings to diatom silica causes the formation of Mg_2Si which results in an altered frustule and distorted pore shapes after HCl and HF treatment.

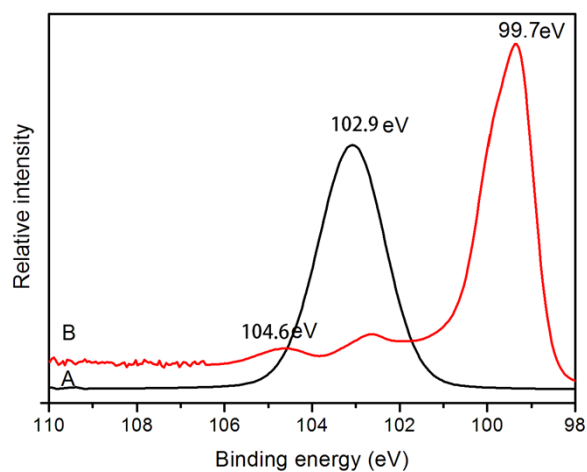


Figure 2S: (A and B) shows Si2p high-resolution XPS data of the diatom *Aulacoseira* sp. frustules before and after magnesiothermic conversion process respectively. Spectrum 2S (A) shows the strong peak at 102.9 eV that confirms the robust Si-O before conversion. The peak at 99.7 eV (Spectrum 2S(B)) shows the silicon peak. The weak peaks at 102.9 eV and 104.6 eV are consistent with residual, superficial Si-O sub-oxides and Si-F species, post HF/HCl treatment.

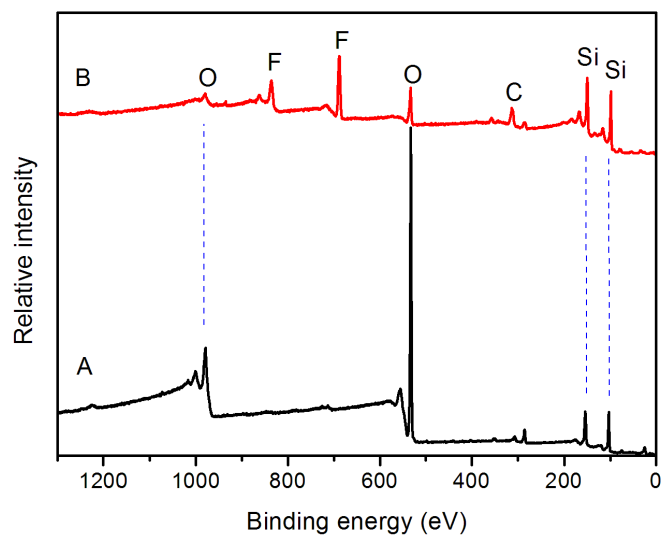


Figure 3S: XPS survey spectra of the diatom *Aulacoseira* sp. frustules before (A) and after (B) magnesiothermic conversion.

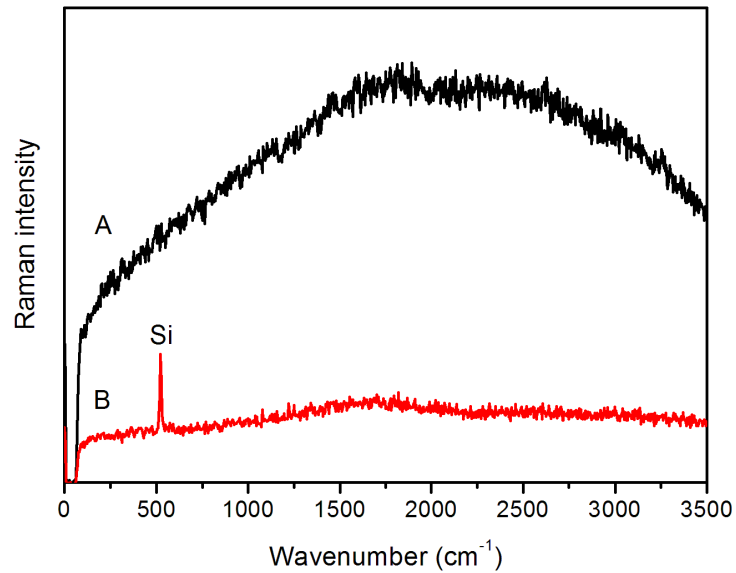


Figure 4S: Raman spectra of the diatom *Aulacoseira* sp. frustules before (A) and after (B) the magnesiothermic conversion. The strong silicon peak at 520 cm⁻¹ in Spectrum (B) further confirms the conversion into silicon when compared to the broad fluorescence background Spectrum (A) from amorphous silica diatom frustules before conversion.

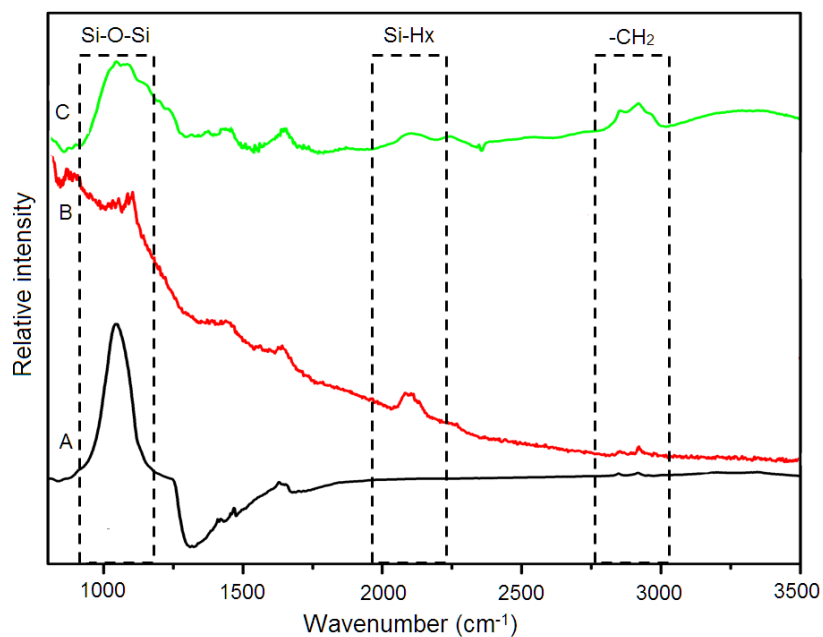


Figure 5S: FTIR spectra of the diatom *Aulacoseira* sp. frustules before (A) and after (B) the magnesiothermic conversion process, and after AM hydrosilylation (C). Spectrum (A) shows the broad stretching peak for Si-O-Si (before conversion) around 1100 cm⁻¹. A Si-H_x stretching peak at 2100 cm⁻¹ was observed after conversion (B).² (C) shows the C-H stretching vibrations around 2900 cm⁻¹, confirming hydrosilylation of the silicon diatom frustule surface.³

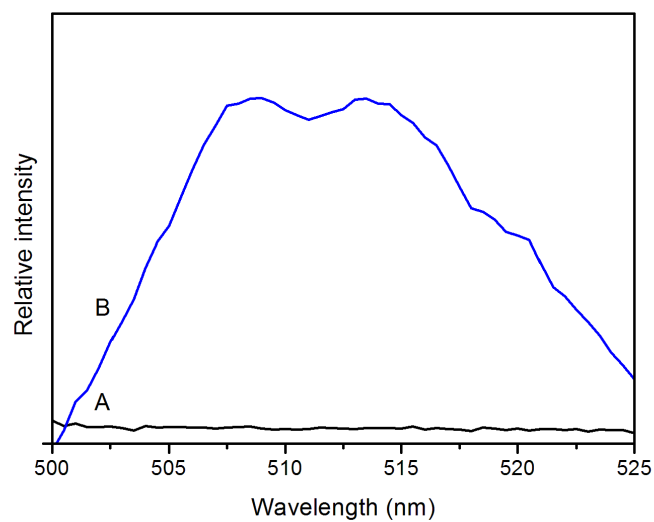


Figure 6S: Fluorescence spectra of silicon diatom frustules (A) and AM hydrosilylated silicon diatom frustules (B) with conjugated fluorescein-5-maleimide dye (498 nm excitation) in PBS buffer at pH 7. The labeling procedure was adapted from.⁴

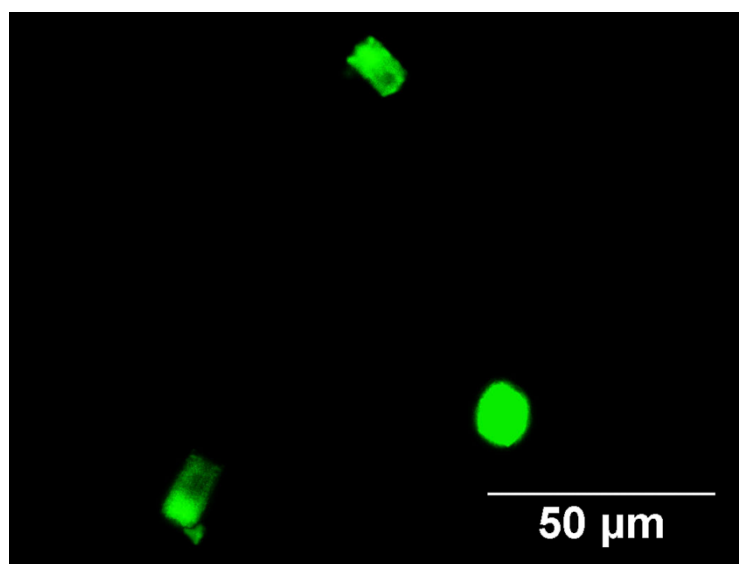


Figure 7S: Fluorescence microscopy images (FITC filter) of AM hydrosilylated silicon diatom frustules.⁴

References:

- 1 Y. Yu, J. Addai-Mensah and D. Losic, *Langmuir*, 2010, **26**, 14068.
- 2 J. Nelles, D. Sendor, A. Ebbers, F. Petrat, H. Wiggers, C. Schulz and U. Simon, *Colloid Polym. Sci.*, 2007, **285**, 729.
- 3 J. Nelles, D. Sendor, F.-M. Petrat and U. Simon, *J. Nanopart. Res.*, 2010, **12**, 1367.
- 4 M. J. Sweetman, C. J. Shearer, J. G. Shapter and N. H. Voelcker, *Langmuir*, 2011, **27**, 9497.